Villa Jorge A. (Orcid ID: 0000-0003-1130-9401)

Plant-mediated methane transport in emergent and floating-leaved species of a temperate freshwater mineral-soil wetland

Jorge A. Villa[1,2*], Yang Ju[1], Taylor Stephen[3], Camilo Rey-Sanchez[1,4], Kelly C. Wrighton[5], Gil Bohrer[1]

[1] Department of Civil, Environmental and Geodetic Engineering. The Ohio State University, Columbus, OH 43210, USA

[2] Now at School of Geosciences. University of Louisiana at Lafayette, Lafayette, LA, 70504, USA

[3] Department of Chemical, Biochemical and Environmental Engineering. University of Maryland – Baltimore County, Baltimore, MD 21250, USA

[4] Now at Department of Environmental Science, Management and Policy. UC Berkeley, CA 94720, USA

[5] Department of Soil and Crop Sciences. Colorado State University, Fort Collins, CO 8523, USA

* Corresponding author: jorge.villa@louisiana.edu

Abstract

Methane flux from freshwater mineral soil (FWMS) wetlands and its variability among sites is largely modulated by plant-mediated transport. However, plant-mediated transport processes are rarely resolved in land surface models and are poorly parametrized for plants commonly found in FWMS wetlands. Here, relationships between methane flux and CO_2 uptake, as well as plant conductance of methane were evaluated for three plant species and two characteristic functional types: emergent (narrow-leaved cattail) and floating-leaved (American lotus and water lily). We found significant but contrasting correlations between methane flux and CO_2 uptake in cattails (*r^2 = 0.51, slope = -0.16*, during morning) and water lily (*r^2 = 0.32, slope = 0.064*, after midday). This relationship was not significant in American lotus, showing that stomata regulation of methane fluxes is species-specific and not generalizable across the floating-leaved plant functional type. Conductance of methane per leaf area showed distinct seasonal dynamics across species. Conductance was similar among the floating-leaved species (6.2×10^{-3} m d^{-1} in lotus and 7.2×10^{-3} m d^{-1} in water lily) and higher than conductance in the emergent species (2.7×10^{-3} m d^{-1}). Our results provide direct observations of plant conductance rates and identify the vegetation parameters (leaf area, stomatal conductance) that modify them. Our results further suggest that models of methane emissions from FWMS should parameterize plant-mediated transport in different

2

plant functional types, scaled by leaf area and with variable seasonal phenological dynamics, and consider possible species-specific mechanisms that control methane transport through plants.

1. Introduction

It is estimated that ~30% of the methane emitted to the atmosphere is produced in wetlands, constituting the single largest natural source (Tian et al. 2016). Freshwater mineral-soil (FWMS) wetlands represent approximately 39% of the global area covered by wetlands, yet they account for up to 65% of the global methane emissions (Bridgham et al. 2006). In North America, it is estimated that FWMS wetlands account for up to 67% of wetland methane emissions (Kolka et al. 2018). However, estimates of methane emissions from these wetlands are still highly variable, in part, because of uncertainties in the rates of plant-mediated transport, which accounts for 30 – 90% of total methane fluxes (Van Der Nat and Middelburg 1998; Ding et al. 2002; Laanbroek 2010; Jeffrey et al. 2019).

Methane is produced in wetland sediments and soils by methanogenic archaea after the stepwise degradation of organic matter under anoxic conditions (Segers 1998). Once produced, methane can be consumed by aerobic methanotrophic bacteria, or can be transported to the surface and emitted to the atmosphere via diffusion, ebullition or plant-mediated transport. Methane transport through wetland plants is the result of an adaptative

3

strategy of most macrophytes to transport oxygen from shoots to roots in order to thrive in

the anoxic environment characteristic of wetland soils. Oxygen is transported as gas flows

through an internal continuum of lacunar spaces formed by aerenchyma tissue connecting

the rhizomes and the leaves (Colmer 2003). The flux in the lacunae is driven by gradients

in pressure and humidity between internal gas spaces and the atmosphere (Dacey 1980;

Dacey 1987; Beckett et al. 1988; Grosse et al. 1991; Tornberg et al. 1994). This

mechanism, known as pressurized ventilation, occurs when oxygen-rich air from the shoots

is vented down through the lacunae. Air with high concentrations of methane, which

diffused into the rhizome from soil porewater, is transported upward and eventually exits

the plant through older leaves, damaged stems or leaves, stomata or micropores in leaf

sheaths (Nouchi et al. 1990; Armstrong and Armstrong 1991; Sorrell and Boon 1994).

Molecular diffusion driven by concentration gradients inside the lacunae is another flux

mechanism driving methane transport (Shannon et al. 1996), although this process is

known to occur at a much lower rate and seems to predominate during the night when

pressurized ventilation is suppressed (Chanton et al. 1993). Additionally, methane that is

dissolved in porewater can be taken up by roots, transported by the sap through the xylem

and eventually transpired through stomata (Nisbet et al. 2009).

  Previous observations have shown large variations in plant-mediated methane transport

rates among species (Sebacher et al. 1983; Joabsson and Christensen 2001; Bhullar et al.

2013). Transport rates may scale with plant biomass (Kankaala et al. 2005; Kao-Kniffin et

al. 2010), phenology (Koebsch et al. 2015), or age (Schütz et al. 1989). Depending on the

4

specific design and regulation of the gas transport mechanisms in different wetland species, methane transport through the plant may be regulated by leaf photosynthesis and stomatal conductance, which are physiologically coupled as plants respond to light and CO_2 concentration and water vapor pressure gradients (Garnet et al. 2005; Matthews and Seymour 2014). Although the role of stomata regulation of methane fluxes has been observed in some plant species (Chanton et al. 1993; Morrissey et al. 1993; Thomas et al. 1996), the relationship between methane flux and carbon dioxide (CO_2) uptake and its variation among species have only be assessed in a few studies (Yavitt and Knapp 1995; Garnet et al. 2005).

Land-surface models that account for methane transport through plants as part of the prognostic process of surface methane flux in wet locations, typically assume a bulk plant-methane-transport conductance coefficient. There are very few observations with which to estimate such coefficients, and most of these are from northern peatlands, and not from FWMS nor from temperate wetlands and their associated plant species. Models diverge in their assumptions and consequent formulation of the type of regulation and dynamics of the plant conductance of methane. In most models, the end result of plant-mediated transport is simulated using a diffusive analogy, multiplying the soil-air concentrations gradient of methane (or some analog of that) by a bulk conductance, i.e. the net conductance of the whole plant system to methane transport from the soil through the plant to the air, and not explicitly resolving within-plant processes such as pressurized ventilation transport or stomatal conductance (Xu et al. 2016). The methane transport conductance parameters for

5

plants may be set to a constant value that represents the overall terrestrial and wetland biomes (Tian et al. 2010; Xu and Tian 2012). In some cases, models assume empirical values for conductance parameters that represent different plant functional types (PFTs) (e.g., the Walter model, Walter and Heimann (2000) or Walter et al. (2001), and in the model ORCHIDEE, Ringeval et al. (2010)). These values are based on the premise that physical traits in plants like root to shoot ratios and root distribution in the soil profile affect methane transport, but without a robust support from direct flux measurements. Alternatively, some models scale the conductance by leaf area, or stem area and stem porosity (CLM4Me, Riley et al. 2011; TRIPLEX-GHG, Zhu et al. 2014).

Aiming for a consistent representation of plant-mediated transport in FWMS wetlands and a better observation-based parametrization of plant transport in modeling efforts to constrain methane fluxes from wetlands ecosystems, we explored the flux rates and possible relationships between methane flux and CO_2 uptake rates in three common temperate FWMS wetland plant species of two different plant functional types: emergent (cattail), and floating-leaved (American lotus and water lily). We predicted that if stomata regulate methane fluxes in any of the species, we would observe a positive correlation during the daytime between methane fluxes and CO_2 uptake. Furthermore, we predicted that bulk conductance of methane would be higher in floating-leaved than in the emergent species given their smaller root to shoot ratios and higher porosity.

2. Methods

6

2.1 Study site

The study was conducted in the Old Woman Creek (OWC), National Estuarine Research Reserve (NERR) in northern Ohio, at the coast of Lake Erie (41°22.758' N, 82° 30.743' W, Figure 1). The OWC is a drowned river-mouth wetland formed on Fluvaquents and Adrian muck soils (Natural Resources Conservation Service, 2017). OWC has a semi-permanent connection with the lake that is constricted by the presence of a semi-porous sand barrier that periodically forms at the wetland's mouth. As a result, a lagoon forms behind the barrier allowing the development of emergent and floating vegetation along the edges of the channel and in elevated deposits from autochthonous organic sources (Bernal and Mitsch 2012). Plant communities in OWC occur following the characteristic microtopographic zonation of most freshwater marshes (Mitsch et al. 2009). There is a zone at shallow and intermittent water levels (i.e., < 30 cm) dominated by emergent vegetation, and a zone with continuous standing water (i.e., > 30 cm) dominated by distinct patches of floating-leaved species. The deeper parts of the wetland along the river channel remain open water. The relative areal distributions of these plant communities show a clear interannual variability as a function of water levels (Whyte et al. 1997; Herdendorf et al. 2006).

2.2. Plant species description

Narrow-leaved cattail (*Typha angustifolia* L.), henceforth cattail, is an erect herbaceous plant with clonal growth, leaves as tall as 230 cm, rhizomes up to 70 cm deep

7

(McNaughton 1966; Grace and Harrison 1986), and root to shoot ratios are typically 1 g g^{-1} d.wt under ambient nutrient levels (Li et al. 2010). Cattail has invasive traits and is common in restored and natural wetlands where it forms dense monostands often outcompeting other species (Fennessy et al. 1994; Tulbure et al. 2007; Cronk and Fennessy 2016). *Nelumbo lutea* (Willd.) Pers (American lotus) is an acaulescent herb, with orbicular flat floating leaves 30– 60 cm in diameter that may emerge from the surface, and short adventitious roots extending from rhizomes that can grow deep in the soil up to 45 cm. *Nymphaeae odorata* Aiton (water lily), is an acaulescent herb as well, with orbicular floating 10–30 cm in diameter leaves and root to shoot ratios around 0.6 g g^{-1} d.w (Richards et al. 2011). Both American lotus and water lily have a widespread distribution through North America (Schneider and Chaney 1981; McNaughton 1966), while cattail has a temperate and circumboreal cosmopolitan distribution. All three species are representative of cosmopolitan genera of macrophytes present in FWMS wetlands. The predominant gas transport mechanism in these species is pressurized ventilation, facilitated by the large and continuous lacunae spaces. In cattails, these spaces consist of a continuous aerenchyma tissue, while in American lotus and water lily of large air tube systems in the stems (Mevi-Schutz and Grosse 1988; Grosse et al. 1991; Chanton 2005).

2.3 Field sampling

2.3.1 *Fluxes through plants*

Methane flux and CO_2 uptake were determined simultaneously by cavity ring-down spectroscopy, using a portable greenhouse gas analyzer (Picarro G4301, Santa Clara, CA) coupled to custom-made leaf chambers (Figure S1). Chambers consisted of transparent plastic storage boxes sealed with rimmed weather stripping and large binder clips. Chambers were fitted with a digital thermometer to monitor and record the temperature inside the chamber. Previous experiments on leaf chambers under sunny conditions indicate that while net photosynthesis is not affected by the time of enclosure despite a significant increase in temperature, changes can occur in methane fluxes and stomatal conductance after 8 minutes of chamber deployment (Knapp and Yavitt 1992). To avoid such effects on stomatal conductance, we deployed our chambers for a conservative total measurement time of 4 minutes during which the chamber is closed. The Gas Scouter recirculates the air within the chamber while monitoring CO_2 and CH_4 concentrations simultaneously at a frequency of 1 Hz. The flow rate of chamber air through the Gas Scouter is ~1 L min^{-1}. The chamber used for sampling cattails had a volume of 3.364 L, and enclosed a section of few leaves, while the volume of the chamber used for American lotuses and water lilies was bigger (12.437 L) allowing for the accommodation of an entire leaf without disruption. In addition, the chamber for floating-leaved species had two floating foams attached outside the chamber that kept it raised above the water level. Samplings were conducted monthly, from June through August 2018.

The sampling period encompassed the macrophyte peak growing season at OWC, aiming to exclude spring and fall transitions of vegetation growth and senescence that could bias

9

the flux measurements. Sampling was conducted in the central portion of the estuary (Figure 1). Every month, we randomly selected 5 adjacent leaves (floating-leaved species) or leaf sections (cattail) at different locations (Figure 1). At each monthly sampling, chambers were deployed at three parts of the day: morning (8:00 to 11:00), midday (13:00 to 15:00) and afternoon (14:00 to 20:00). The morning time period included the peak in methane emissions (around 8:30 am), previously identified by Rey-Sanchez et al. (2018) in the sampling site. During each monthly campaign, we conducted the sampling of one species during a single day, except for June, when we sampled American lotus and water lily at the same day and cattail at the next day. Chambers were placed on the same leaves during the morning, midday and afternoon of the same day. These leaves were harvested at the end of the day. Chambers in cattails were placed 50 cm above the water surface, which was within the upper 2/3 of the leaves (Yavitt and Knapp 1995) and included 5 replicates of 4 – 6 leaf sections arrays at each enclosure. The sheath of the cattail leaves that we sampled was below the water level in all samplings. Measurements in American lotuses and water lilies were conducted on single floating leaves at 5 replicates as well. The leaves we sampled were already directly exposed to the atmosphere (i.e., not submerged). For gas flux measurements, the leaves were raised from the water surface and isolated in the chamber. After the sampling we checked for visible mechanical damage to the leaves that may have been caused during the daily sampling and thus compromised the sampling. We did not have to replace any measurement due to damage to leaves.

2.3.2 *Leaf area*

10

We measured the one-sided leaf area directly enclosed by the chamber by harvesting the leaves we sampled. We used one-sided leaf area because in the floating-leaf species methane flux to the air is done through the upper side of the leaf that is exposed to the air. Furthermore, one-sided leaf area is the standard vegetation property observed from remote sensing. To scale the flux from per leaf area in the chamber to flux per ground area for the plant type we also estimated the general leaf area index (LAI, $m^2 \, m^{-2}$) of each species after each diurnal sampling using a $0.25 \, m^2$ PVC frame (5 replicates) in the immediate area where we sampled. For American lotuses and water lilies, we took digital photographs that were processed to measure the proportion of area covered by leaves and then normalized by the area of the frame. We did not account for overlapping leaf areas as we assumed that submerged covered leaves do not participate actively in the exchange of gases with the atmosphere. Accordingly, the possible maximum LAI measured in floating-leaved species was 1. For cattails, we harvested the leaves inside the frame, clipping them at the water surface level, bagged and transported the leaves to the laboratory for further processing. Leaves from the June sampling were carefully measured to determine the area, then dried and weighted to generate an empirical allometric equation of specific leaf area to estimate LAI (unitless, m^2 leaf/m^2 ground) as a function of dry weight, W, (g) (LAI = $51W/A_f$ + 12.1, $r^2 = 0.93$, $p < 0.001$, where A_f is the sample frame area, $0.25 \, m^2$). We used this function to approximate the cattail LAI for July and August as a function of the dry weight of harvested biomass samples. We assumed that this allometric relationship between LAI

11

and dry weight did not significantly change during the peak growing season (Weisner 1993).

2.3.1 *Dissolved-gas porewater concentrations*

We measured methane porewater concentrations at ten depths from five *in-situ* dialysis samplers (peepers, MacDonald et al. 2013) deployed throughout the sampling area (Figure 1). Each peeper consisted of ten, 61.4 ml, vertically spaced, inner cells. The distance between cells was 5.6 cm. Peeper cells were filled with DI water before deployment and after each sampling. Dissolved gases in the porewater diffused into the inner-cells through a polyethersulfon membrane with 0.22-µm pore size. 10 ml subsamples from the cells were collected through a hosing system connected to each cell and placed in glass vials holding 0.2 ml of 1M HCl to prevent microbial activity in the vial. Vials were filled to the top, crimped and kept refrigerated until processing (see MacDonald et al. (2013) for full details on sampler design, deployment, and operation). Once in the laboratory, concentrations of dissolved methane were obtained using the GC headspace equilibration technique (Kampbell et al. 1989). We used a 3-ml subsample from each vial to equilibrate in a 57-ml headspace of nitrogen.

The peepers represent a minimally disruptive way of sampling porewater and typically could be resampled on a frequency of once per 2 weeks or longer. Peepers were sampled within 2 days before the leaf-chamber samples. Unlike the gas-fraction concentration in the air, dissolved methane concentration in the porewater is changing slowly. Furthermore, the peepers equilibrate with the porewater concentration through a dialysis filter membrane and

12

take about 1-2 weeks to equilibrate fully. The peeper measurements, therefore, represent a

slow (~10 days) moving average of the porewater concentration of dissolved gasses during

the same time that instantaneous leaf-level fluxes were measured.

   Peepers in our site were installed 1 or 2 years prior to this sampling campaign (Angle et

al. 2017) and though the vegetation cover type changes between growing seasons, we did

not move the peepers to minimize the disturbance to the sediments. We assumed that the

mean porewater concentration observed in two peepers under a particular vegetation type

was representative of this patch type throughout the central section of the wetland. The

northernmost peeper, C1 (Figure 1) currently located near the edge of a cattail patch, was

originally placed near the center of a cattail-dominated area that started transitioning to

American lotus in April-May 2018. When we sampled, the vegetation cover of this peeper

comprised mostly dead cattail shoots and sparse lotus leaves. For our analyses, we assigned

the observed porewater concentrations from this peeper as characteristic to cattails.

Because we could not reposition the peepers, we were limited in our ability to adjust

porewater sampling locations in response to changes in vegetation patch locations. We also

do not know the vertical root-density distributions of the different plant species and

therefore used a uniform vertical average of porewater concentrations over the peepers'

depth. Because of these limitations, the assumption that porewater concentration in the

peepers under each patch type is representative of the concentration experienced by each of

that patch's plants is associated with large uncertainty. We address this uncertainty with an

upper-bound uncertainty estimate using the vertical and lateral variation among all

13

porewater measurements (see more details of uncertainty estimates and their calculation approach in section 2.6 below).

2.4 Methane flux and conductance through plants

In each chamber measurement, we fitted the 4 minute, 1 Hz time series of methane or CO_2 concentrations, C_{HM} (µmol mol^{-1}), to the non-linear Hutchinson and Moiser one-dimension diffusion model (Hutchinson and Mosier 1981; Kutzbach et al. 2007; Pedersen et al. 2010):

$$C_{HM} = C_s + (C_0 - C_s) e^{-kt} \tag{1}$$

Where C_0 is the pre-deployment concentration of methane or CO_2 (µmol mol^{-1}), C_s is the constant source or sink concentration (µmol mol^{-1}), and k is a curve shape parameter (s^{-1}). C_0, C_s, and k are determined by fitting the observed gas concentrations in the chamber over time, t (s), to eq. 1. We then calculated the flux, F, of methane and CO_2, F_{CH4} and F_{CO2}, respectively, (µmol m$_{leaf}^{-2}$ s^{-1}) at the leaf surface as:

$$F = k \ (C_0 - C_s) \ \frac{p \, V}{R \, Tch \, A} \tag{2}$$

Where p (Pa) is the atmospheric pressure, measured at a nearby eddy covariance tower (Ameriflux site ID: US-OWC, Bohrer 2018); V the volume of the chamber (m^3), R the universal gas constant (8.314 m^3 Pa mol^{-1} K^{-1}), Tch the temperature inside the chamber (K) and A the area of the leaf enclosed in the chamber (m^2).

14

Examples for our flux calculation approach and quality control are provided in Figure S2. Out of the 135 flux measurements, we discarded 31 where the goodness of fit for C_{HM} was lower than 0.9 ($r^2 < 0.9$) in either methane flux or CO_2 uptake. Discarded data were evenly distributed among species and did not show discernible patterns with the times of the day or month of sampling, except for measurements of cattails in June during morning time, which were all discarded (Table S1).

The apparent patch-level bulk plant conductance of methane from the soil to the atmosphere per leaf area, $CH_4 conductance$ (m d^{-1}), was calculated for each plant species as (after, Yavitt and Knapp 1995 and Nouchi et al. 1994):

$$CH_4 conductance = \frac{F_{CH4}}{(C_{soil} - C_{air})} \ 86400 \qquad (3)$$

Where C_{soil} (µmol m^{-3}) is the methane porewater concentration at the day of sampling, calculated as the vertical average of the 10 peepers cells within the rooting zone (depths of 0 – 50 cm), in two peepers at the soil under each plant species (one for Cattail). C_{air} (µmol m^{-3}) is the equivalent aqueous concentration of methane in the air, and 86400 is the number of seconds in one day.

We calculated C_{air} as:

$$C_{air} = C_{ch} p H^{cp} \qquad (4)$$

Where C_{ch} (µmol mol^{-1}) is the average 5 methane concentration measurements in each chamber deployment, p (Pa) is the atmospheric pressure and H^{cp} the Henry's solubility constant for methane (1.4×10^{-5} mol m^{-3} Pa^{-1}).

15

We estimated plant conductance of methane per ground area by multiplying $CH_4 conductance$ by the species-specific LAI. All data for and results of the conductance calculation are presented in Table S1 and Table S3. The conductance we measure is the instantaneous conductance, averaged during 4 minutes of the chamber measurements. While it does not represent a daylong measurement, we chose to report it in m d^{-1} to keep consistency with the units reported in the literature and explicitly used in some land surface models (e.g. DLEM).

It is also important to note that this apparent patch-level bulk conductance is not exactly and exclusively the conductance of a particular plant tissue (root, stem, and leaf) to the movement of dissolved or gas-phase methane. Instead, it represents an assumed effective bulk conductance for movement of methane between the soil and the air though a pathway that typifies the vegetation within a certain ecosystem patch. In other words, it is the bulk conductance that models that do not explicitly resolve methane movement within the plants use to parameterize the plant flow contribution. We, therefore, do not calculate conductance values for individual plants but combine the patch-level mean plant-flow-through flux, the mean porewater concentration over an assumed and equally distributed rooting depth, and the mean leaf area to calculate the apparent bulk conductance. We scale the conductance by leaf area as it is the most easily measurable characteristic of any vegetated patch. We choose not to scale conductance by the stem or xylem diameter, or by vegetation height as these are typically unknown for particular patches at high (weekly) temporal resolution. Furthermore, the conductance we report represents the conductance of methane that is

16

flowing through leaf blades exposed to the atmosphere, not accounting for methane that is diffused through the water column, even though some methane may enter the water column through the submerged parts of the plants. In this experiment, we particularly focused on flux from the plants to the air, and not of diffusive flux from the water column, as the latter is more commonly measured and reported for wetlands using floating chambers and modeled using a different parallel pathway of emission.

2.5 Relations between methane and carbon fluxes

To test whether methane flux is regulated by stomatal conductance we measured the significance of a linear regression between methane flux and CO_2 flux (CO_2 uptake rate is driven by stomatal conductance) for each species. We hypothesize that if stomata control methane flux, the observed rate of methane flux in a chamber should be positively correlated with the rate of carbon uptake in the same chamber, as carbon uptake is, to a large degree and particularly during the day, controlled by stomata conductance. The regressions were performed pooling data across samples for the morning observations, midday and afternoon observations, and the overall combined diurnal sampling period. This grouping of the observations is driven by the assumption that methane accumulation at night when stomata are closed may flush out when stomata open in the morning and thus stomata-methane flux relationships in the morning may present different patterns than during the rest of the day.

17

2.6 Uncertainty analysis for conductance of methane through plants

We made two major assumptions in our patch-level bulk conductance calculations with regards to the concentration gradients (the denominator of the conductance calculation, eq. 3). One is that the effective concentration controlling the diffusion of methane from the sediments to the roots system is uniform throughout the vertical extent of the top 50 cm of the sediment profile. This assumption is equivalent to assuming the rooting-depth distribution is uniform at depths between 0 and 50 cm. The other assumption we made is that vertically averaged porewater concentrations are spatially homogeneous within each vegetation type and represented by the small sample of peepers in that patch. We estimated the maximal uncertainty associated with the vertical heterogeneity of porewater concentrations by recalculating the conductance using the lowest and highest porewater concentrations along the sediment profile at each vegetation type and sampling. We estimated the maximal uncertainty associated with the spatial heterogeneity of methane porewater concentration by recalculating methane conductance using the lowest and highest vertically averaged porewater concentrations at any given location in the entire site. For both uncertainty estimates, we used the range between the highest and lowest observed concentrations, rather than the standard deviation of the observations, to provide upper bounds to the uncertainty estimates.

2.7 Data analysis and availability

18

We processed data and conducted regression tests and fit models using MATLAB®
2018b. We used JMP 14® Pro 14.0.0 for all other statistical tests. All the statistical tests
were conducted at a 0.05 significance level. We used Wilcoxon paired comparisons to test
the differences between methane fluxes during different times of the day. To test the
hypothesis of different conductance of methane in plant functional types we used an ordinal
logistic model with conductance as the response variable, plant species as the fixed effect
and month of sampling nested by plant species. We used the same model setup to test for
differences in CO_2 uptake at the leaf level for the plant species during the three samplings.

Meteorological data for the measurement site at Old Woman Creek are available through
the National Estuarine Research Centralized Data Management Office
(http://cdmo.baruch.sc.edu/get/landing.cfm), and through the Ameriflux site US-OWC
(Bohrer 2015, https://ameriflux.lbl.gov/sites/siteinfo/US-OWC). Surface chamber
measurements and porewater concentrations for OWC, including these used in this study
are available through The Department of Energy data portal - ESS-DiVE (Bohrer et al
2019, https://data.ess-dive.lbl.gov/view/doi:10.15485/1568865).

3. Results and discussion

3.1 Species-specific mechanisms of plant methane transport regulation

Median (and interquartile range) foliar methane fluxes for cattail (0.13 (0.032 – 0.61)
µmol m_{leaf}^{-2} s^{-1}), were within the range reported for cattails in several wetlands of different
climates in the USA (0.01 – 1.49 µmol m_{leaf}^{-2} s^{-1}, mean 0.22 µmol m_{leaf}^{-2} s^{-1}, Yavitt and

Knapp 1995). Similarly, foliar fluxes from American lotus (0.34 (0.085 – 0.58) µmol m_{leaf}^{-2} s^{-1}) and water lily (0.47 (0.079 – 0.8) µmol m_{leaf}^{-2} s^{-1}) agree well with fluxes reported in other studies (0.2 –1.8 µmol m_{leaf}^{-2} s^{-1}) for wetland plants common in FWS wetlands with pressurized ventilation and diffusion-driven flow (Garnet et al. 2005). We did not find statistical differences among the fluxes during different times of the day for any of the plant species (Figure 2b, d, f), although observations in cattail were more variable in the morning and showed distinct higher observations extremes in the mid-to-late morning (Figure 2a). Diurnal dynamics in plant methane flux were previously attributed to the gas transport mechanism (Chanton et al. 1993) and the regulating role of photosynthesis and stomatal conductance in gas exchange (White and Ganf 2000; Garnet et al. 2005; Matthews and Seymour 2014), which are in turn dependent of variations in temperature and irradiance (Knapp and Yavitt 1995; Whiting and Chanton 1996). Garnet et al. (2005) estimated that stomatal conductance and net CO_2 assimilation accounted for up to half of the variation in methane flux among four wetland species of different life traits, although the effect of stomatal conductance was three times that of equivalent changes in CO_2 assimilation. Ruling out the effect of different transport mechanisms, they attributed the remaining variability to temperature, plant physical differences, such as the root surface area involved in methane uptake, and slow processes that operate at time scales exceeding the hourly scales, such as rhizosphere oxidation of methane or root carbon exudation.

We found negative correlations between methane flux and carbon uptake rates in cattails during the morning, and positive correlations between methane flux and carbon uptake

20

rates in water lily during the afternoon and overall (Figure 3). While correlation does not infer causation, strong mechanistic regulation of methane flux by stomata will lead to an apparent positive correlation between methane flux and carbon uptake, as they will both share a common regulatory mechanism. However, such a positive correlation could be misleading if methane and carbon flux are both correlated to other environmental drivers, for example temperature, soil moisture, or light. Yet, during the growing season, daytime temperatures do not limit photosynthesis, and thus, are not strongly correlated with daytime carbon uptake rate (Labate and Leegood 1988). Further, wetland soil are essentially always flooded and thus photosynthesis in the wetland does not decrease due to water shortage (Farquhar and Sharkey 1982). Finally, photosynthesis and carbon uptake are controlled by light level, but light level is not expected to directly affect methane flux. Therefore, varying light levels during the daily measurements' times could add noise and obscure a stomata-driven correlation between carbon and methane fluxes, but light-level variations cannot generate a spurious positive correlation.

   In cattail species, Yavitt and Knapp (1995) proposed that during the night when stomata are closed, and pressurized ventilation is negligible, soil-to-plant methane concentration gradients drive the diffusion of methane into the rhizome and from there to lower parts of the leaf. At sunrise, stomata open and pressurized ventilation driven by temperature and humidity gradients between leaves and air resumes, fluxing out the methane, which has been accumulating during the night. Typically, methane fluxes exhibit a large transient peak at mid-to-late morning (e.g., Rey-Sanchez et al. 2019), associated with increasing

21

light levels (Whiting and Chanton 1996). Later throughout the day, as methane

concentration in the leaves decrease, methane fluxes become limited by pressurized

ventilation and not by stomata conductance. Whiting and Chanton (1996) reasoned that the

apparent control of stomata during the morning must be circumstantial after observing that

the morning peak of methane flux occurred before the peak in stomatal conductance, which

occurred later at midday. They argued that the initial opening of stomata allowed the

release of methane explaining the peak in the morning, when light levels, and therefore CO_2

uptake rates, are low. Instead of functioning as a flux regulator, stomata function as a

"release valve" for methane upon the initial opening. Our results indeed show a significant

negative correlation between methane flux through cattail and CO_2 uptake during the

morning, but not throughout the rest of the day (Figure 3a, d, g), agreeing with this release

valve hypothesis.

The flux of methane and its possible relationship with CO_2 uptake in floating-leaved

species is less understood than it is for cattails. We found a significant correlation between

methane flux and CO_2 uptake in water lily (Figure 3i). When breaking the measurements by

the time of the day, the correlation was only observed after midday (Figure 3f), when

photosynthetic yields are at its maximum (Ritchie 2012), which strongly supports the

assumption that methane is regulated by stomatal conductance in this species. However, a

definite confirmation of a mechanistic link would require actual simultaneous

measurements of stomatal conductance (i.e., Garnet et al. 2005). Interestingly, we did not

find any correlation between methane flux and CO_2 uptake for the American lotus (Figure

22

3b,e, h). Unlike other macrophytes, the flow of gases in lotus is actively regulated by large

stomata found in the center of the leaves. These stomata, different from those found in leaf

blades, open in the morning, close at midday and reopen late in the afternoon, decreasing

conductance in response to increasing light (Matthews and Seymour 2014). Possibly, the

large central stomata do not account for the bulk of photosynthesis (Dacey 1987). This

would decouple the CO_2 uptake observations from the conductance of these stomata that

control methane flux, and lead to the apparent lack of correlation between methane flux and

carbon uptake.

   Overall, the data indicate that the relationship between methane flux and CO_2 uptake is

different between the floating-leaved and emergent species. We found a contrasting

correlation between cattail and water lily, and at different times of the day. However, our

observations failed to show similarity in the methane-carbon flux relationship among the

two floating-leaved species, showing that stomata regulation of methane fluxes is not

necessarily generalizable to FWMS wetland species according to their growth-form

characterization of PFT.

3.2 Conductance of methane is different among emergent and floating-leaved species

   As expected, median (and interquartile range) methane conductance during the three

month study period was similar in the floating-leaved species (*p = 0.27*), 6.2×10^{-3} (1.8×10^{-3}

$- 1.1\times10^{-2}$) m d^{-1} and 7.2×10^{-3} ($1.2\times10^{-3} - 1.6\times10^{-2}$) m d^{-1}, in lotus and water lily,

respectively, and these significantly differed from that of the cattail (*p = 0.003*), an

23

emergent species, 2.7×10^{-3} m d^{-1} ($6.2 \times 10^{-4} - 9.8 \times 10^{-3}$) (Figure 4a). On top of the observed variability in methane conductance throughout the study period, we found high uncertainty due to vertical heterogeneity of methane porewater concentrations. Our estimates indicate that uncertainty may account for up to $40 - 67\%$ lower and $137 - 284\%$ higher conductance (depending on species) than the median conductance values we report. This uncertainty due to the vertical concentration variations was considerably higher than the uncertainty due to the spatial heterogeneity of the mean profile concentrations (estimated to account for between $8 - 34\%$ lower and $11 - 93\%$ higher, depending on species) (Table S2). Overall, the uncertainty associated with vertical and spatial heterogeneity of methane concentration in the soil is within the range of the observed variability of conductance. Therefore, we believe that such uncertainty does not obscure the actual values that our observations represent.

   In general, our observations of conductance are low, and at or somewhat below the low end of the range reported by other studies based on partial field measurements or estimated from modeling approaches. For instance, DLEM, one of the available models capable of simulating plant-mediated methane transport uses a default conductance value of 0.68 m d^{-1}, selected as a median value from a range of $8 \times 10^{-3} - 17.2$ m d^{-1} reported in the literature (Tian et al. 2010; Xu et al. 2015). That median value is much higher than the average median value we observed for the two floating-leaved species (6.7×10^{-3} m d^{-1}) and the median value we observed for the cattail (2.7×10^{-3} m d^{-1}). Nonetheless, the values we observed are near the lower edge of the previously reported range. Our values were also an

24

order of magnitude lower than the estimates for rice (3.5×10^{-2} m d^{-1}, Nouchi et al. 1994) and considerably lower than previously assumed conductance for cattail (1.78 m d^{-1}, Yavitt and Knapp, 1995). The differences between our measurements and values measured in rice and assumed/observed in peatland PFTs may be due to the high porosity of peat soils that reduce the resistance of transport from soil to root (in the case of peatlands), or due to anatomical differences between plants species, such as xylem porosity or root to shoot length ratios (Smirnoff and Crawford 1983; Tornberg et al. 1994; Lorenzen et al. 2001; Richards et al. 2011).

The different plant species had distinct seasonal dynamics (Figure 4a). In cattails, the median (and interquartile range) conductance per leaf area increase as the season progressed, from 3.8×10^{-4} (1.5×10^{-4} – 5.1×10^{-4}) m d^{-1} in June to 7.6×10^{-3} (1.6×10^{-3} – 1.2×10^{-2}) m d^{-1} in August. In contrast, conductance decreased in lotus from 9.6×10^{-3} (6.5×10^{-3} m d^{-1} – 1.2×10^{-2}) m d^{-1} to 2.6×10^{-3} (9.3×10^{-4} – 8×10^{-3}), while in lily peaked and was more variable in July 1.91×10^{-3} (7×10^{-3} – 3.2×10^{-2}) m d^{-1}. Seasonal variations in methane conductance through cattails could be associated with the controlling role of biomass in the pressurized ventilation. Convective throughflow in cattails is thought to initiate at the top parts of the leaves, where atmospheric humidity is relatively low, whereas internal air with methane is vented from lower parts of the leaves or older leaves in the culm (Yavitt and Knapp 1998). As the leaves grow taller, their potential for pressurized ventilation increases. Rising heights could explain our observations of more significant methane fluxes towards the middle and end of summer when the plants were taller, and thus

25

their LAI was larger (Figure 4b). Alternatively, the increase in conductance may be related to overall plant aging and the occurrence of senesced areas with larger pores that enhance flux by increasing conductance (Sebacher et al. 1985; Schütz et al. 1989; Constable et al. 1992). Seasonal peaks as observed in water lily may be explained, at least in part, by the direct link between methane flux and photosynthesis (Figure 3i). Water lilies have relatively high photosynthetic yields (Ritchie 2012), and the total photosynthetically active radiation during midday in the days we sampled water lilies peaked during July and drastically declined by the sampling in August due to cloud cover (Figure S3).

   When stomata are open, the limiting step in plant methane conductance is the diffusion of methane from the soil to the rhizomes (Beckett et al. 2001; Ding et al. 2004; Henneberg et al. 2012). Remarkably, we did not find a significant difference between species or during the season within species in per-leaf-area CO_2 fluxes (Figure 5b). However, although we found variations in methane porewater concentrations throughout the sampling period, none of the seasonal dynamics in plant flow-through fluxes followed the seasonal pattern of porewater variation (Figure 5a, Table S3). It is possible that the high concentrations in porewater in our site, have supported constant high concentrations of methane in the lacunae, despite the seasonal variations. The porewater concentrations we found at OWC are 3-20 times higher than the commonly reported in other wetland ecosystems (Chasar et al. 2000; Elberling et al. 2011; Wang et al. 2018). If variations in porewater methane concentrations were not driving seasonal methane plant flow-through fluxes, then

26

morphological and physiological differences in conductance among plant species must account for the seasonal-scale variability we observed in methane fluxes.

4. Conclusions and implications for modeling

Poor representation of plant conductance in process-based methane models is an important source of variability in model outputs (Tang et al. 2010). Our results offer valuable insights that could help improve the modeling of plant-mediated transport of methane in FWMS wetlands. The bulk patch-level conductance we report is estimated at a scale equivalent with the resolution at which models define plant transport processes and therefore the values we report could be directly used to constrain parameterizations in similar wetlands and vegetation types. To our knowledge, methane conductance through floating-leaved species has not been evaluated before, nor applied explicitly in models. Most of the parameters used in current methane models come from modeling approaches evaluated against measurements in rice (Sigren et al. 1997) or estimations in PFTs, such as grass, rushes, sedges, reeds or mosses, characteristic to and observed at peatlands and not FWMS wetlands. Such values are typically derived from modeling approaches based on principles of transport and kinetics (Van Den Pol-Van Dasselaar et al. 1999; Segers and Leffelaar 2001a; Segers and Leffelaar 2001b; Kettunen 2003), which to date have been applied with very limited field data (Walter and Heimann, 2000; Walter et al. 2001). Our observations suggest a lower bulk conductance of methane than previously reported for individual plants. It is important to note that the porewater concentration of methane at our

27

site was up to 10 times higher than the concentrations reported by other studies that measured conductance (Nouchi et al. 1994; Yavitt and Knapp, 1995), though the flux rates we observed were higher, but at a similar scale to other's observations. If the flux is not increasing linearly with porewater concentration but increases more slowly at high concentrations (for example, if it follows a logarithmic curve), conductances at high concentration sites will be lower than at low concentration sites. More observations of porewater concentration, methane flux, and derived bulk conductances across many sites are needed to determine this possibility. Overall, our observations provide an important source of directly measured values of apparent bulk conductance in FWMS plant functional types and indicate that parameter values used in models should not be generalized across all wetland and plant functional types.

It is easy for models to assume constant parameters for conductance per leaf area and scale methane conductance per ground area from plant species following dynamic diagnosis or prescribed seasonally variable LAI. However, our results revealed significant intra-seasonal variations in methane conductance per leaf area in the three plant species (Figure 4a). Future efforts should focus on pinning down the environmental and plant-physiological drivers of this change and developing the algorithms that allow including the seasonal dynamics of methane conductance in plant-mediated transport sub-models.

As our results indicate, generalizing and including a plant-mediated transport mechanism into land-surface models based only on the correlation between methane flux and CO_2 uptake is implausible given the strong differences between species in the apparent

28

relationship between methane and CO_2 fluxes. Including a stomatal-conductance-dependent transport mechanism into models would require detailed knowledge of the diurnal variation of methane fluxes and the role (or lack thereof) of stomata conductance in controlling methane fluxes in different species. Diurnal variation and stomata regulation of methane is currently known only in some species and unfortunately, as our results suggest, would not necessarily follow a growth-form based PFT classification.

Nonetheless, the use of stomatal-regulated methane fluxes could represent a valuable foundation towards a more physiologically realistic representation of plant-mediated transport mechanisms for some species in future or existing mechanistic models that simulate methane biogeochemistry in spatially distributed columns and work on sub-daily time steps. The spatial distribution could comprise the ecosystem scale (e.g., *ecosys,* Grant and Roulet 2002; Chang et al. 2019) or the regional scale (e.g., CLM4Me, Riley et al. 2011). With some assumptions about the shape of the daily cycle of methane conductance, it could potentially be integrated into models that work on a daily scale as well, such as wetlands DNDC (Zhang et al. 2002; Taft et al. 2019). Splitting wetlands from a single assumed 'wetland' type patch to multiple patches (or sub-grid-scale tiles) of the different plant functional types that compose the whole site will require a PFT-based parameterization. As we show, PFT classification that follows the growth form of wetland plants does not necessarily capture the functional type with regard to the regulation of methane fluxes. It is possible that wetland PFTs would have to be defined based on the combination of growth form and mechanisms of methane transport regulation. This may

29

lead to an unmanageably large number of PFTs. However, given that plant zonation in most FWMS wetlands tends to be dominated by a small number of species, the parametrization can potentially be done for species with the distinction between stomata-regulated and non-stomata-regulated methane transporting species.

Besides *N. odorata* (in this study), other plant species common to FWMS wetlands, such as *Carex spp.* (Morrissey et al. 1993; Schimel 1995), *Orontium aquaticum*, *Peltandra virgnica*, *Juncus effusus*, (Garnet et al. 2005), and *Scirpus lacustris* (Van Der Nat and Middelburg 1998) show stomata-regulated methane fluxes. Species identification could be done using traditional sampling and collection, but recent developments in remote sensing techniques, coupling high-resolution multi-spectral imagery with machine learning are making this task less field intensive (Dronova et al. 2012; Carle et al. 2014).

Our results also suggest that incorporating methane conductance in current models based on plant functional type could help improve the representation of plant-mediated transport, at least for FWMS wetlands. For example, if we were to simulate methane emissions from FWMS wetlands in North America using a model such as DLEM in an approach similar to that presented by Xu & Tian (2012), choosing the median methane conductance that we found for the cattail species, instead of the median for the floating-leaved species, will lead to a two-fold underestimation of plant-mediated methane transport (assuming that methane concentration in the soil is the same). Although limited in the number of species evaluated, the possible sensitivity to the plant methane conductance parameter in models warrants at the very least, the need of more measurements to probe more robustly the difference in

30

conductance between emergent and floating leaved-species (and possibly among other PFTs) and their causes, and to understand the underlying spatial and temporal structure of the variation of conductance among regions, wetlands, seasons and species.

References

Angle, J. C., T. H. Morin, L. M. Solden, and others. 2017. Methanogenesis in oxygenated soils is a substantial fraction of wetland methane emissions. Nat. Comm. **8**: 1567. doi:10.1038/s41467-017-01753-4

Armstrong, J., and W. Armstrong. 1991. A convective through-flow of gases in *Phragmites australis* (Cav.) Trin. ex Steud. Aquat. Bot. **39**: 75–88. doi:10.1016/0304-3770(91)90023-X

Beckett, P. M., W. Armstrong, and J. Armstrong. 2001. Mathematical modelling of methane transport by *Phragmites*: the potential for diffusion within the roots and rhizosphere. Aquat. Bot. **69**: 293–312.

Beckett, P. M., W. Armstrong, S. H. F. W. Justin, and J. Armstrong. 1988. On the relative importance of convective and diffusive gas flows in plant aeration. New Phytol. **110**: 463–468. doi:10.1111/j.1469-8137.1988.tb00283.x

Bernal, B., and W. J. Mitsch. 2012. Comparing carbon sequestration in temperate freshwater wetland communities. Glob. Chang. Biol. **18**: 1636–1647. doi:10.1111/j.1365-2486.2011.02619.x

Bhullar, G. S., M. Iravani, P. J. Edwards, and H. Olde Venterink. 2013. Methane transport and emissions from soil as affected by water table and vascular plants. BMC Ecology **13**: 32. doi:10.1186/1472-6785-13-32

Bohrer, G. 2018. AmeriFlux US-OWC Old Woman Creek. http://dx.doi.org/10.17190/AMF/1418679.

32

Bohrer G ; Ju Y ; Arend K ; Morin T ; Rey-Sanchez C ; Wrighton K ; Villa J.2019)
Methane and CO2 chamber fluxes and porewater concentrations US-OWC
Ameriflux wetland site, 2015-2018. AmeriFlux Management Project.
doi:10.15485/1568865

Bridgham, S., J. Megonigal, J. Keller, N. Bliss, and C. Trettin. 2006. The carbon balance of
North American wetlands. Wetlands **26**: 889-916–916.

Carle, M. V., L. Wang, and C. E. Sasser. 2014. Mapping freshwater marsh species
distributions using WorldView-2 high-resolution multispectral satellite imagery. Int.
J. Remote Sens. **35**: 4698–4716. doi:10.1080/01431161.2014.919685

Chang, K.-Y., W. J. Riley, P. M. Crill, R. F. Grant, V. I. Rich, and S. R. Saleska. 2019.
Large carbon cycle sensitivities to climate across a permafrost thaw gradient in
subarctic Sweden. The Cryosphere **13**: 647–663. doi:https://doi.org/10.5194/tc-13-
647-2019

Chanton, J. P. 2005. The effect of gas transport on the isotope signature of methane in
wetlands. Org. Geochem. **36**: 753–768. doi:doi: 10.1016/j.orggeochem.2004.10.007

Chanton, J. P., G. J. Whiting, J. D. Happell, and G. Gerard. 1993. Contrasting rates and
diurnal patterns of methane emission from emergent aquatic macrophytes. Aquat.
Bot. **46**: 111–128. doi:10.1016/0304-3770(93)90040-4

Chasar, L. S., J. P. Chanton, P. H. Glaser, and D. I. Siegel. 2000. Methane concentration
and stable isotope distribution as evidence of rhizospheric processes: comparison of

33

a Fen and Bog in the Glacial Lake Agassiz Peatland Complex. Ann. Bot. **86**: 655–663. doi:10.1006/anbo.2000.1172

Colmer, T. D. 2003. Long-distance transport of gases in plants: a perspective on internal aeration and radial oxygen loss from roots. Plant, Cell Environ. **26**: 17–36. doi:10.1046/j.1365-3040.2003.00846.x

Constable, J. Y. H., J. B. Grace, and D. J. Longstreth. 1992. High carbon dioxide concentrations in aerenchyma of *typha latifolia*. Am. J. Bot. **79**: 415–418. doi:10.1002/j.1537-2197.1992.tb14568.x

Cronk, J. K., and M. S. Fennessy. 2016. Wetland plants: biology and ecology, CRC press.

Dacey, J. W. H. 1980. Internal winds in water lilies: an adaptation for life in anaerobic sediments. Science **210**: 1017–1019.

Dacey, J. W. H. 1987. Knudsen-transitional flow and gas pressurization in leaves of *Nelumbo*. Plant Physiol. **85**: 199. doi:10.1104/pp.85.1.199

Ding, W., Z. Cai, and H. Tsuruta. 2004. Diel variation in methane emissions from the stands of *Carex lasiocarpa* and *Deyeuxia angustifolia* in a cool temperate freshwater marsh. Atmos. Environ. **38**: 181–188. doi:10.1016/j.atmosenv.2003.09.066

Ding, W., Z. Cai, H. Tsuruta, and X. Li. 2002. Effect of standing water depth on methane emissions from freshwater marshes in northeast China. Atmos. Environ. **36**: 5149–5157. doi:10.1016/S1352-2310(02)00647-7

Dronova, I., P. Gong, N. E. Clinton, L. Wang, W. Fu, S. Qi, and Y. Liu. 2012. Landscape analysis of wetland plant functional types: The effects of image segmentation scale, vegetation classes and classification methods. Remote Sens. Environ. **127**: 357–369. doi:10.1016/j.rse.2012.09.018

Elberling, B., L. Askaer, C. J. Jørgensen, H. P. Joensen, M. Kühl, R. N. Glud, and F. R. Lauritsen. 2011. Linking soil O_2, CO_2, and CH_4 concentrations in a wetland soil: implications for CO_2 and CH_4 fluxes. Environ. Sci. Technol. **45**: 3393–3399. doi:10.1021/es103540k

Farquhar, G. D., and T. D. Sharkey. 1982. Stomatal Conductance and Photosynthesis. Annu. Rev. Plant. Physiol. **33**: 317–345. doi:10.1146/annurev.pp.33.060182.001533

Fennessy, M. S., J. K. Cronk, and W. J. Mitsch. 1994. Macrophyte productivity and community development in created freshwater wetlands under experimental hydrological conditions. Ecol. Eng. **3**: 469–484. doi:10.1016/0925-8574(94)00013-1

Garnet, K. N., J. P. Megonigal, C. Litchfield, and G. E. Taylor. 2005. Physiological control of leaf methane emission from wetland plants. Aquat. Bot. **81**: 141–155. doi:10.1016/j.aquabot.2004.10.003

Grace, J. B., and J. S. Harrison. 1986. The biology of Canadian weeds.: 73. *Typha latifolia* L., *Typha angustifolia* L. and *Typha xglauca* Godr. Can. J. Plant Sci. **66**: 361–379.

Grant, R. F., and N. T. Roulet. 2002. Methane efflux from boreal wetlands: Theory and testing of the ecosystem model Ecosys with chamber and tower flux measurements. Global Biogeochem. Cycles **16**: 2–1. doi:10.1029/2001GB001702

Grosse, W., H. Bernhard Büchel, and H. Tiebel. 1991. Pressurized ventilation in wetland plants. Aquat. Bot. **39**: 89–98. doi:10.1016/0304-3770(91)90024-Y

Henneberg, A., B. K. Sorrell, and H. Brix. 2012. Internal methane transport through *Juncus effusus*: experimental manipulation of morphological barriers to test above-and below-ground diffusion limitation. New Phytol . **196**: 799–806.

Herdendorf, C. E., D. M. Klarer, and R. C. Herdendorf. 2006. The Ecology of Old Woman Creek, Ohio: An Estuarine and Watershed Profile, 2nd Ed. Ohio Department of Natural Resources.

Hutchinson, G., and A. Mosier. 1981. Improved Soil Cover Method for Field Measurement of Nitrous Oxide Fluxes 1. Soil Sci. Soc. Am. J. **45**: 311–316.

Jeffrey, L. C., D. T. Maher, S. G. Johnston, B. P. Kelaher, A. Steven, and D. R. Tait. 2019. Wetland methane emissions dominated by plant-mediated fluxes: Contrasting emissions pathways and seasons within a shallow freshwater subtropical wetland. Limnol. Oceanogr.

Joabsson, A., and T. R. Christensen. 2001. Methane emissions from wetlands and their relationship with vascular plants: an Arctic example. Glob. Change Biol. **7**: 919–932. doi:10.1046/j.1354-1013.2001.00044.x

36

Kampbell, D. H., J. T. Wilson, and S. A. Vandegrift. 1989. Dissolved oxygen and methane in water by a GC headspace equilibration technique. I. J. Environ. Anal. Chem. **36**: 249–257. doi:10.1080/03067318908026878

Kankaala, P., T. Käki, S. Mäkelä, A. Ojala, H. Pajunen, and L. Arvola. 2005. Methane efflux in relation to plant biomass and sediment characteristics in stands of three common emergent macrophytes in boreal mesoeutrophic lakes. Glob. Change Biol. **11**: 145–153. doi:10.1111/j.1365-2486.2004.00888.x

Kao-Kniffin, J., D. S. Freyre, and T. C. Balser. 2010. Methane dynamics across wetland plant species. Aquat. Bot. **93**: 107–113. doi:10.1016/j.aquabot.2010.03.009

Kettunen, A. 2003. Connecting methane fluxes to vegetation cover and water table fluctuations at microsite level: A modeling study. Global Biogeochem. Cycles **17**. doi:10.1029/2002GB001958

Knapp, A. K., and J. B. Yavitt. 1992. Evaluation of a closed-chamber method for estimating methane emissions from aquatic plants. Tellus B **44**: 63–71. doi:10.3402/tellusb.v44i1.15425

Knapp, A. K., and J. B. Yavitt. 1995. Gas exchange characteristics of *Typha latifolia* L. from nine sites across North America. Aquat. Bot. **49**: 203–215. doi:10.1016/0304-3770(94)00433-M

Koebsch, F., G. Jurasinski, M. Koch, J. Hofmann, and S. Glatzel. 2015. Controls for multi-scale temporal variation in ecosystem methane exchange during the growing season

of a permanently inundated fen. Agric. For. Meteorol. **204**: 94–105.

doi:10.1016/j.agrformet.2015.02.002

Kolka, R., C. Trettin, K. Krauss, and others. 2018. Chapter 13: Terrestrial wetlands, p. 507–
567. *In* Second State of the Carbon Cycle Report (SOCCR2): A Sustained
Assessment Report. U.S. Global Change Research Program.

Kutzbach, L., J. Scneider, T. Sachs, and others. 2007. CO_2 flux determination by closed-
chamber methods can be seriously biased by inappropriate application of linear
regression. Biogeosciences **4**: 1005–1025.

Laanbroek, H. J. 2010. Methane emission from natural wetlands: interplay between
emergent macrophytes and soil microbial processes. A mini-review. Ann. Bot. **105**:
141–153. doi:10.1093/aob/mcp201

Labate, C. A., and R. C. Leegood. 1988. Limitation of photosynthesis by changes in
temperature. Planta **173**: 519–527. doi:10.1007/BF00958965

Li, S., J. Lissner, I. A. Mendelssohn, H. Brix, B. Lorenzen, K. L. McKee, and S. Miao.
2010. Nutrient and growth responses of cattail (Typha domingensis) to redox
intensity and phosphate availability. Ann. Bot. **105**: 175–184.
doi:10.1093/aob/mcp213

Lorenzen, B., H. Brix, I. A. Mendelssohn, K. L. McKee, and S. L. Miao. 2001. Growth,
biomass allocation and nutrient use efficiency in *Cladium jamaicense* and *Typha
domingensis* as affected by phosphorus and oxygen availability. Aquat. Bot. **70**:
117–133. doi:10.1016/S0304-3770(01)00155-3

MacDonald, L. H., J. S. Paull, and P. R. Jaffé. 2013. Enhanced semipermanent dialysis samplers for long-term environmental monitoring in saturated sediments. Environ. Monit. Assess. **185**: 3613–3624. doi:10.1007/s10661-012-2813-8

Matthews, P. G. D., and R. S. Seymour. 2014. Stomata actively regulate internal aeration of the sacred lotus *Nelumbo nucifera*. Plant, Cell Environ. **37**: 402–413. doi:10.1111/pce.12163

McNaughton, S. J. 1966. Ecotype function in the *Typha* community-type. Ecol. Monogr. **36**: 297–325. doi:10.2307/1942372

Mevi-Schutz, J., and W. Grosse. 1988. A two- way gas transport system in *Nelumbo nucifera*. Plant, Cell Environ. **11**: 27–34.

Mitsch, W. J., J. G. Gosselink, C. J. Anderson, and L. Zhang. 2009. Wetland ecosystems, John Wiley & Sons.

Morrissey, L. A., D. B. Zobel, and G. P. Livingston. 1993. Significance of stomatal control on methane release from *Carex*-dominated wetlands. Chemosphere **26**: 339–355. doi:10.1016/0045-6535(93)90430-D

Natural Resources Conservation Service, U.S. Department Of Agriculture. 2017. Web Soil Survey.

Nisbet, R. E. R., R. Fisher, R. H. Nimmo, and others. 2009. Emission of methane from plants. Proc. R. Soc. B **276**: 1347–1354.

Nouchi, I., S. Mariko, and K. Aoki. 1990. Mechanism of methane transport from the rhizosphere to the atmosphere through rice plants. Plant Physiol. **94**: 59. doi:10.1104/pp.94.1.59

Nouchi, I., T. Hosono, K. Aoki, and K. Minami. 1994. Seasonal variation in methane flux from rice paddies associated with methane concentration in soil water, rice biomass and temperature, and its modelling. Plant and Soil **161**: 195–208. doi:10.1007/BF00046390

Pedersen, A. R., S. O. Petersen, and K. Schelde. 2010. A comprehensive approach to soil-atmosphere trace-gas flux estimation with static chambers. Eur. J. Soil Sci. **61**: 888–902. doi:10.1111/j.1365-2389.2010.01291.x

Richards, J. H., T. G. Troxler, D. W. Lee, and M. S. Zimmerman. 2011. Experimental determination of effects of water depth on *Nymphaea odorata* growth, morphology and biomass allocation. Aquat. Bot. **95**: 9–16. doi:10.1016/j.aquabot.2011.03.002

Riley, W., Z. Subin, D. Lawrence, S. Swenson, M. Torn, L. Meng, N. Mahowald, and P. Hess. 2011. Barriers to predicting changes in global terrestrial methane fluxes: analyses using CLM4Me, a methane biogeochemistry model integrated in CESM. Biogeosciences **8**: 1925–1953.

Ringeval, B., N. de Noblet-Ducoudré, P. Ciais, P. Bousquet, C. Prigent, F. Papa, and W. B. Rossow. 2010. An attempt to quantify the impact of changes in wetland extent on methane emissions on the seasonal and interannual time scales. Global Biogeochem. Cycles **24**: n/a-n/a. doi:10.1029/2008GB003354

Ritchie, R. J. 2012. Photosynthesis in the blue water lily (*Nymphaea caerulea* Saligny) using pulse amplitude modulation fluorometry. Int. J. Plant Sci. **173**: 124–136. doi:10.1086/663168

Schimel, J. P. 1995. Plant transport and methane production as controls on methane flux from arctic wet meadow tundra. Biogeochemistry **28**: 183–200. doi:10.1007/BF02186458

Schneider, E. L., and T. Chaney. 1981. The floral biology of *Nymphaea odorata* (*Nymphaeaceae*). The Southwestern Naturalist **26**: 159–165. doi:10.2307/3671112

Schütz, H., W. Seiler, and R. Conrad. 1989. Processes involved in formation and emission of methane in rice paddies. Biogeochemistry **7**: 33–53. doi:10.1007/BF00000896

Sebacher, D. I., R. C. Harriss, and K. B. Bartlett. 1983. Methane flux across the air-water interface: air velocity effects. Tellus B **35B**: 103–109. doi:10.1111/j.1600-0889.1983.tb00014.x

Sebacher, D. I., R. C. Harriss, and K. B. Bartlett. 1985. Methane emissions to the atmosphere through aquatic plants1. J. Environ. Qual. **14**: 40–46.

Segers, R. 1998. Methane production and methane consumption: a review of processes underlying wetland methane fluxes. Biogeochemistry **41**: 23–51. doi:10.1023/A:1005929032764

Segers, R., and P. A. Leffelaar. 2001a. Modeling methane fluxes in wetlands with gas-transporting plants: 1. Single-root scale. Journal of Geophysical Research: Atmospheres **106**: 3511–3528.

Segers, R., and P. A. Leffelaar. 2001b. Modeling methane fluxes in wetlands with gas-transporting plants: 3. Plot scale. J. Geophys. Res.: Atmos. **106**: 3541–3558. doi:10.1029/2000JD900482

Shannon, R. D., J. R. White, J. E. Lawson, and B. S. Gilmour. 1996. Methane efflux from emergent vegetation in peatlands. J. Ecol. **84**: 239–246.

Sigren, L., G. Byrd, F. Fisher, and R. Sass. 1997. Comparison of soil acetate concentrations and methane producton, transport, and emission in two rice cultivars. Global Biogeochem. Cycles **11**: 1–14.

Smirnoff, N., and R. M. M. Crawford. 1983. Variation in the structure and response to flooding of root aerenchyma in some wetland plants. Ann. Bot. **51**: 237–249. doi:10.1093/oxfordjournals.aob.a086462

Sorrell, B. K., and P. I. Boon. 1994. Convective gas flow in *Eleocharis sphacelata* R. Br.: methane transport and release from wetlands. Aquat. Bot. **47**: 197–212. doi:10.1016/0304-3770(94)90053-1

Taft, H. E., P. A. Cross, A. Hastings, J. Yeluripati, and D. L. Jones. 2019. Estimating greenhouse gases emissions from horticultural peat soils using a DNDC modelling approach. J. Environ. Manage. **233**: 681–694. doi:10.1016/j.jenvman.2018.11.113

Thomas, K. L., J. Benstead, K. L. Davies, and D. Lloyd. 1996. Role of wetland plants in the diurnal control of CH_4 and CO_2 fluxes in peat. Soil Biol. Biochem. **28**: 17–23. doi:10.1016/0038-0717(95)00103-4

Tian, H., C. Lu, P. Ciais, and others. 2016. The terrestrial biosphere as a net source of greenhouse gases to the atmosphere. Nature **531**: 225.

Tian, H., X. Xu, M. Liu, W. Ren, C. Zhang, G. Chen, and C. Lu. 2010. Spatial and temporal patterns of CH_4 and N_2O fluxes in terrestrial ecosystems of North America during 1979–2008: application of a global biogeochemistry model. Biogeosciences **7**: 2673–2694.

Tornberg, T., M. Bendix, and H. Brix. 1994. Internal gas transport in *Typha latifolia* L. and *Typha angustifolia* L. 2. Convective throughflow pathways and ecological significance. Aquat. Bot. **49**: 91–105.

Tulbure, M. G., C. A. Johnston, and D. L. Auger. 2007. Rapid Invasion of a Great Lakes Coastal Wetland by Non-native *Phragmites australis* and *Typha*. J. Great Lakes Res. **33**: 269–279. doi:10.3394/0380-1330(2007)33[269:RIOAGL]2.0.CO;2

Van Den Pol-Van Dasselaar, A., M. L. Van Beusichem, and O. Oenema. 1999. Determinants of Spatial Variability of Methane Emissions from Wet Grasslands on Peat Soil. Biogeochemistry **44**: 221–237.

Van Der Nat, F.-J. W. A., and J. J. Middelburg. 1998. Effects of two common macrophytes on methane dynamics in freshwater sediments. Biogeochemistry **43**: 79–104. doi:10.1023/A:1006076527187

Walter, B. P., and M. Heimann. 2000. A process-based, climate-sensitive model to derive methane emissions from natural wetlands: Application to five wetland sites,

sensitivity to model parameters, and climate. Global Biogeochem. Cycles **14**: 745–765. doi:10.1029/1999GB001204

Walter, B. P., M. Heimann, and E. Matthews. 2001. Modeling modern methane emissions from natural wetlands 1. Model description and results. J. Geophys. Res. **106**: 34189–34206. doi:10.1029/2001JD900165

Wang, W., C. Zeng, J. Sardans, C. Wang, C. Tong, and J. Peñuelas. 2018. Soil methane production, anaerobic and aerobic oxidation in porewater of wetland soils of the Minjiang River Estuarine, China. Wetlands **38**: 627–640. doi:10.1007/s13157-018-1006-9

Weisner, S. E. B. 1993. Long-term competitive displacement of *Typha latifolia* by *Typha angustifolia* in a eutrophic lake. Oecologia **94**: 451–456.

White, S. D., and G. G. Ganf. 2000. Influence of stomatal conductance on the efficiency of internal pressurisation in *Typha domingensis*. Aquat. Bot. **67**: 1–11. doi:10.1016/S0304-3770(99)00090-X

Whiting, G. J., and J. P. Chanton. 1996. Control of the diurnal pattern of methane emission from emergent aquatic macrophytes by gas transport mechanisms. Aquat. Bot. **54**: 237–253.

Whyte, R. S., D. A. Francko, and D. M. Klarer. 1997. Distribution of the floating-leaf macrophyte *Nelumbo lutea* (American water lotus) in a coastal wetland on Lake Erie. Wetlands **17**: 567–573. doi:10.1007/BF03161523
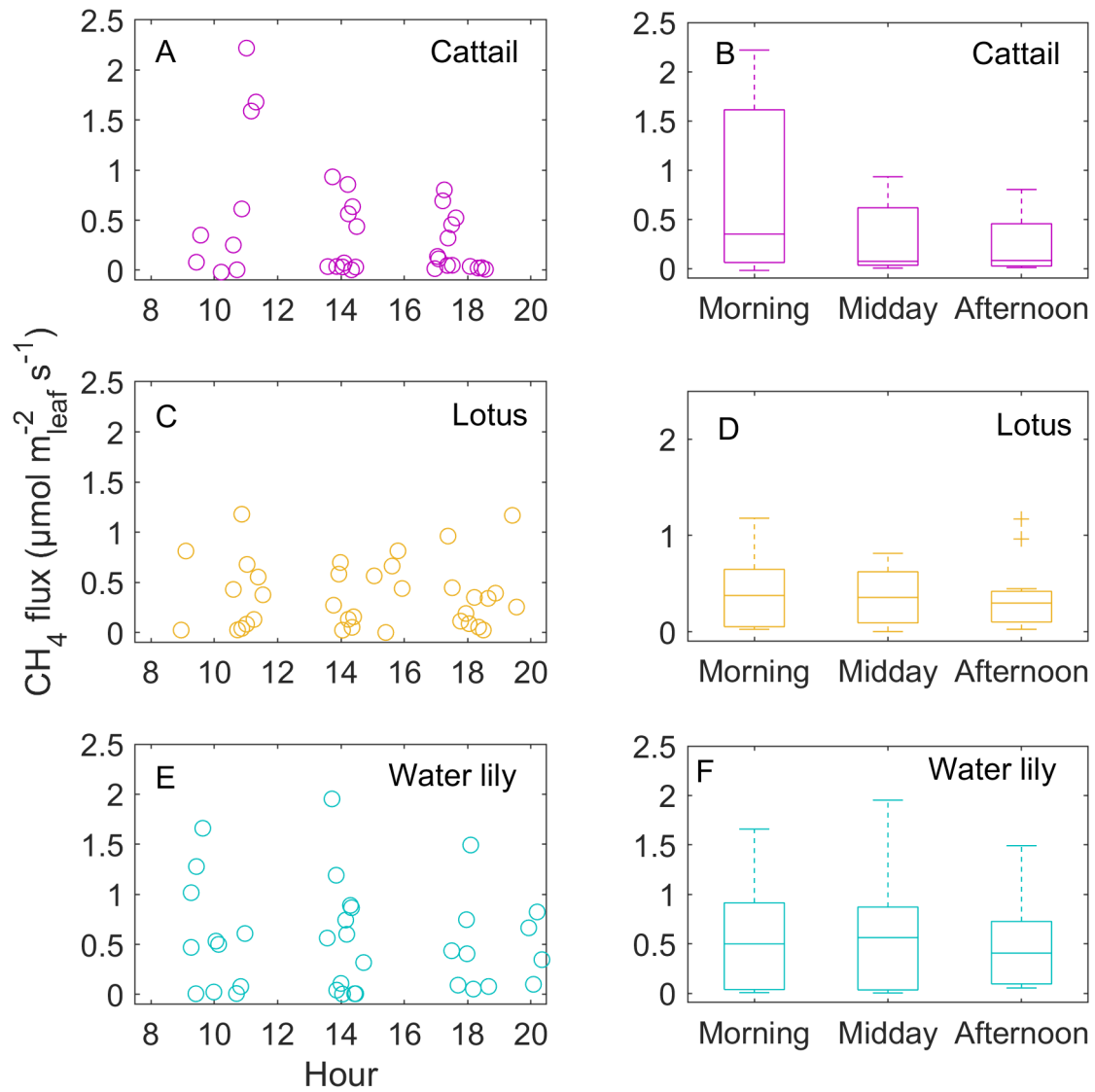
Xu, X., D. A. Elias, D. E. Graham, T. J. Phelps, S. L. Carroll, S. D. Wullschleger, and P. E. Thornton. 2015. A microbial functional group-based module for simulating methane production and consumption: Application to an incubated permafrost soil. Biogeosciences **120**: 1315–1333. doi:10.1002/2015JG002935

Xu, X., and H. Tian. 2012. Methane exchange between marshland and the atmosphere over China during 1949–2008. Global Biogeochem. Cycles **26**. doi:10.1029/2010GB003946

Xu, X., F. Yuan, P. J. Hanson, and others. 2016. Reviews and syntheses: four decades of modeling methane cycling in terrestrial ecosystems. Biogeosciences **13**: 3735–3755.

Yavitt, J. B., and A. K. Knapp. 1995. Methane emission to the atmosphere through emergent cattail (*Typha latifolia* L.) plants. Tellus B **47**: 521–534. doi:10.3402/tellusb.v47i5.16065

Yavitt, J. B., and A. K. Knapp. 1998. Aspects of methane flow from sediment through emergent cattail (*Typha latifolia*) plants. New Phytol. **139**: 495–503.

Zhang, Y., C. Li, C. C. Trettin, H. Li, and G. Sun. 2002. An integrated model of soil, hydrology, and vegetation for carbon dynamics in wetland ecosystems. Global Biogeochem. Cycles **16**: 1061.

Zhu, Q., J. Liu, C. Peng, and others. 2014. Modelling methane emissions from natural wetlands by development and application of the TRIPLEX-GHG model. Geoscientific Model Development **7**: 981–999.
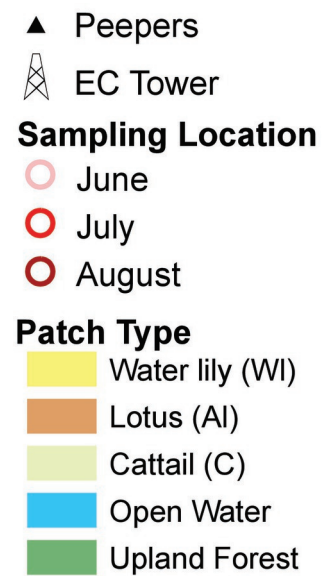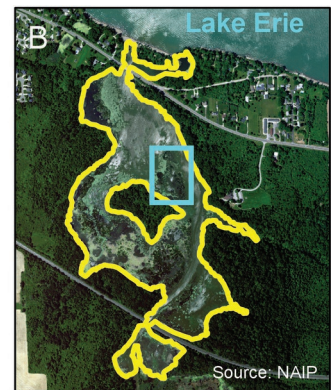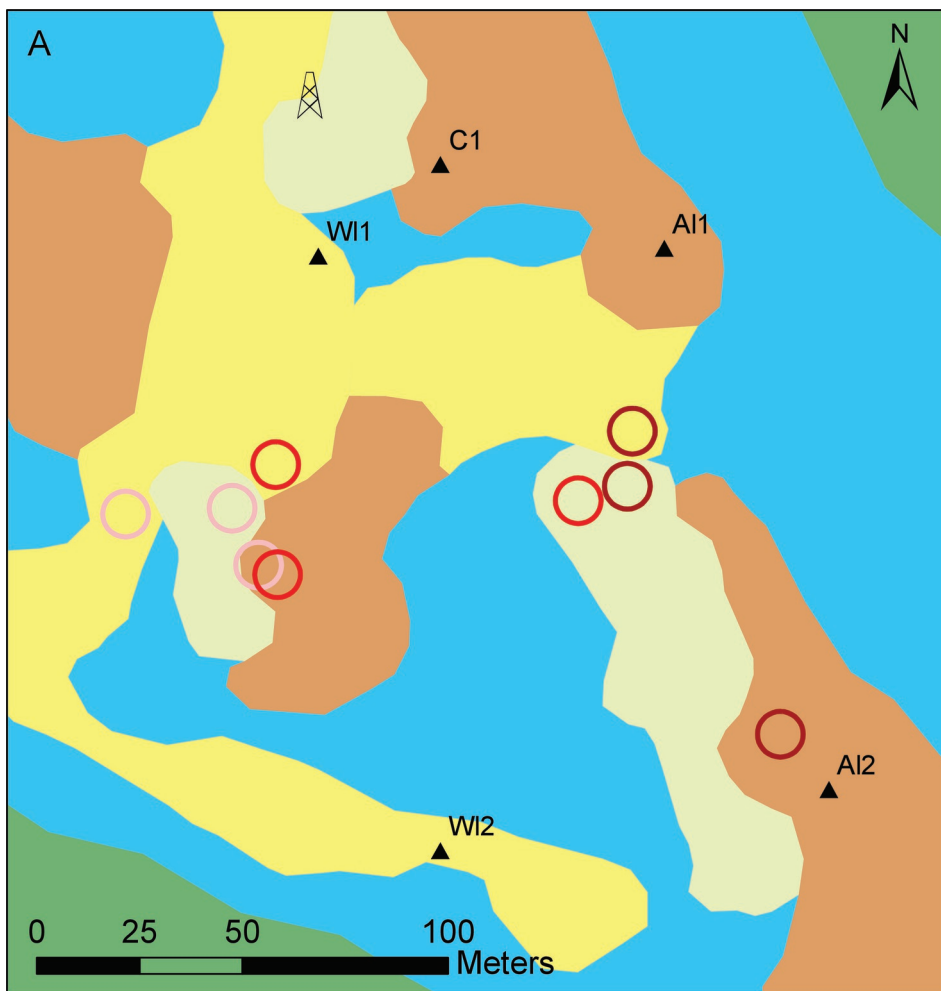
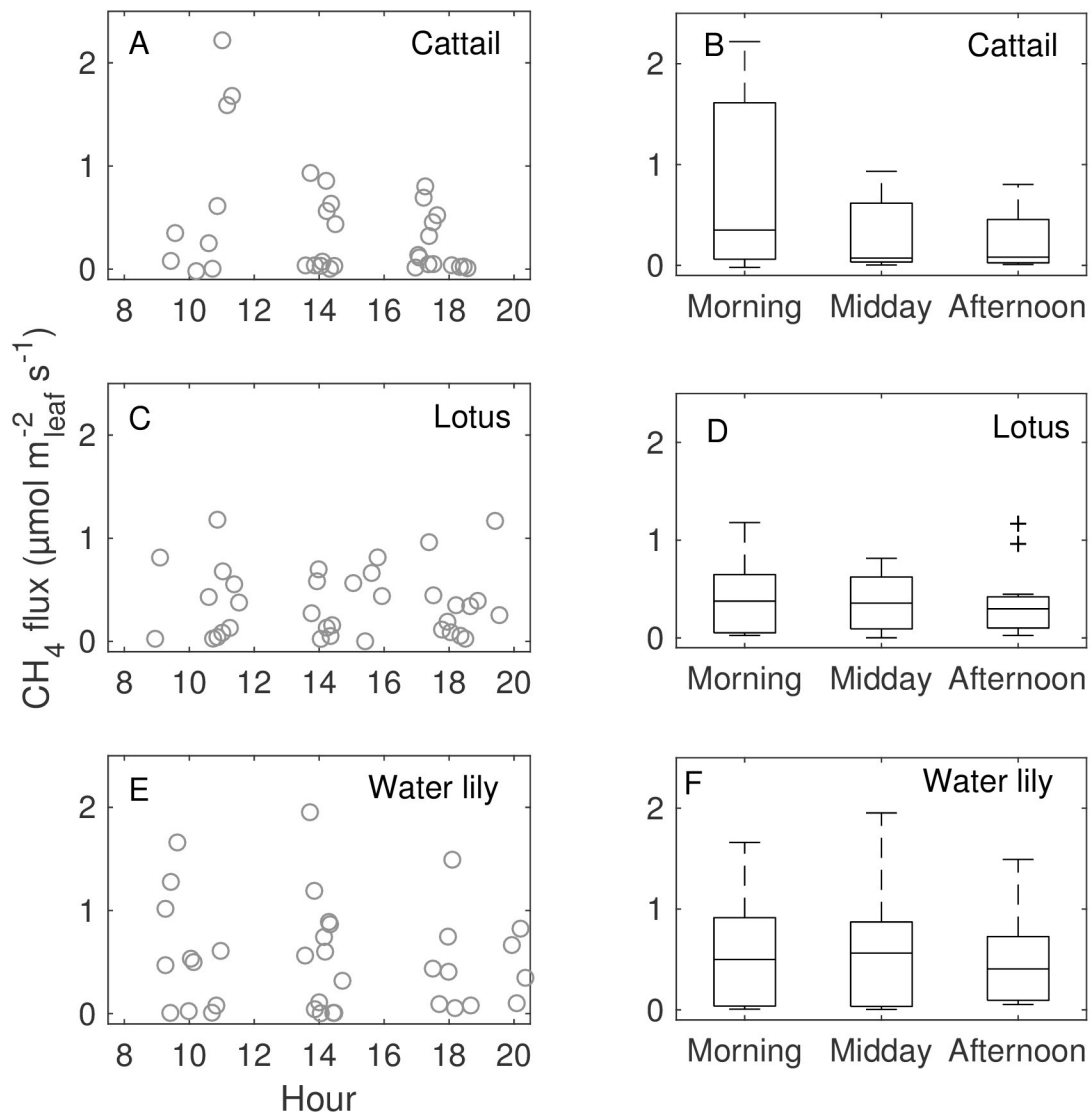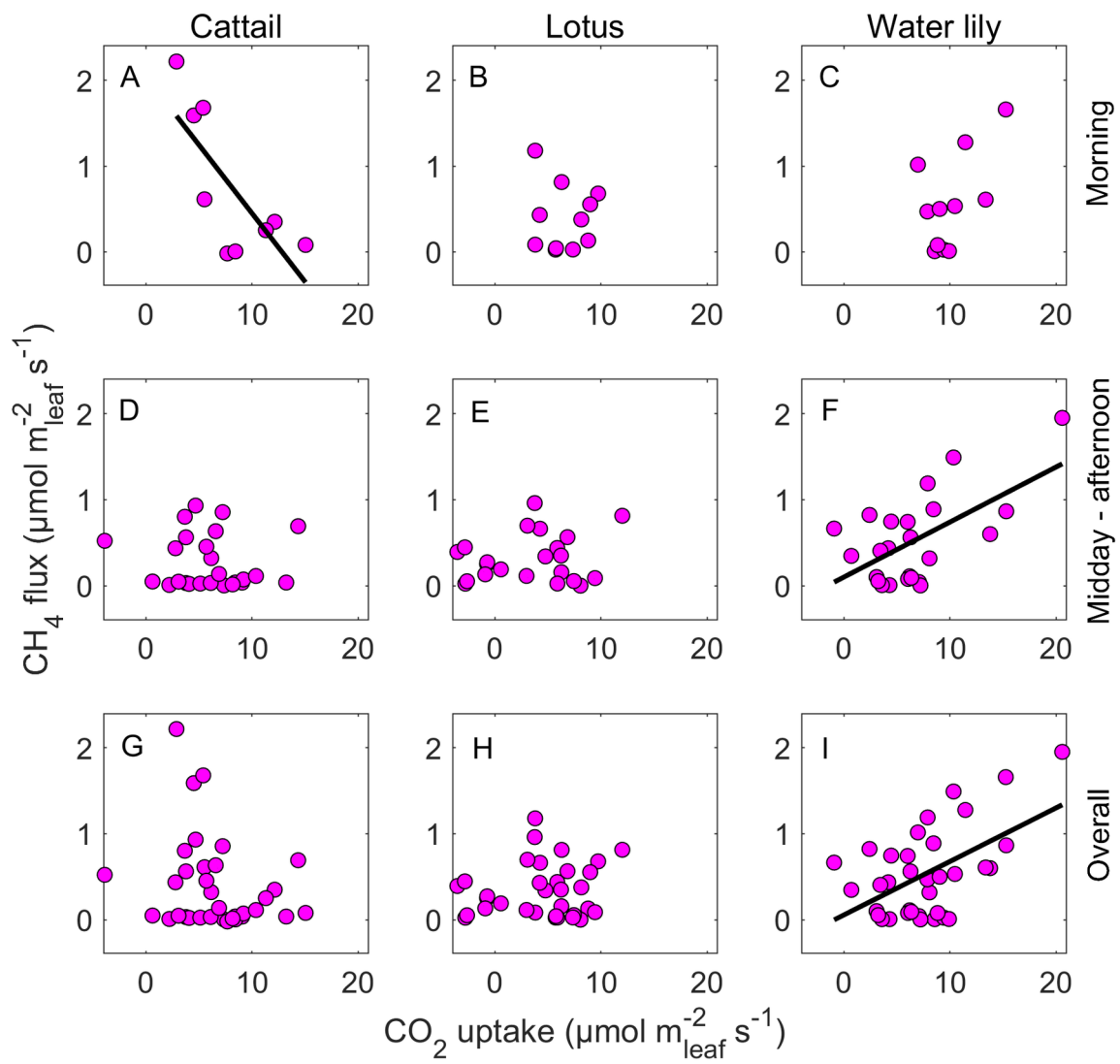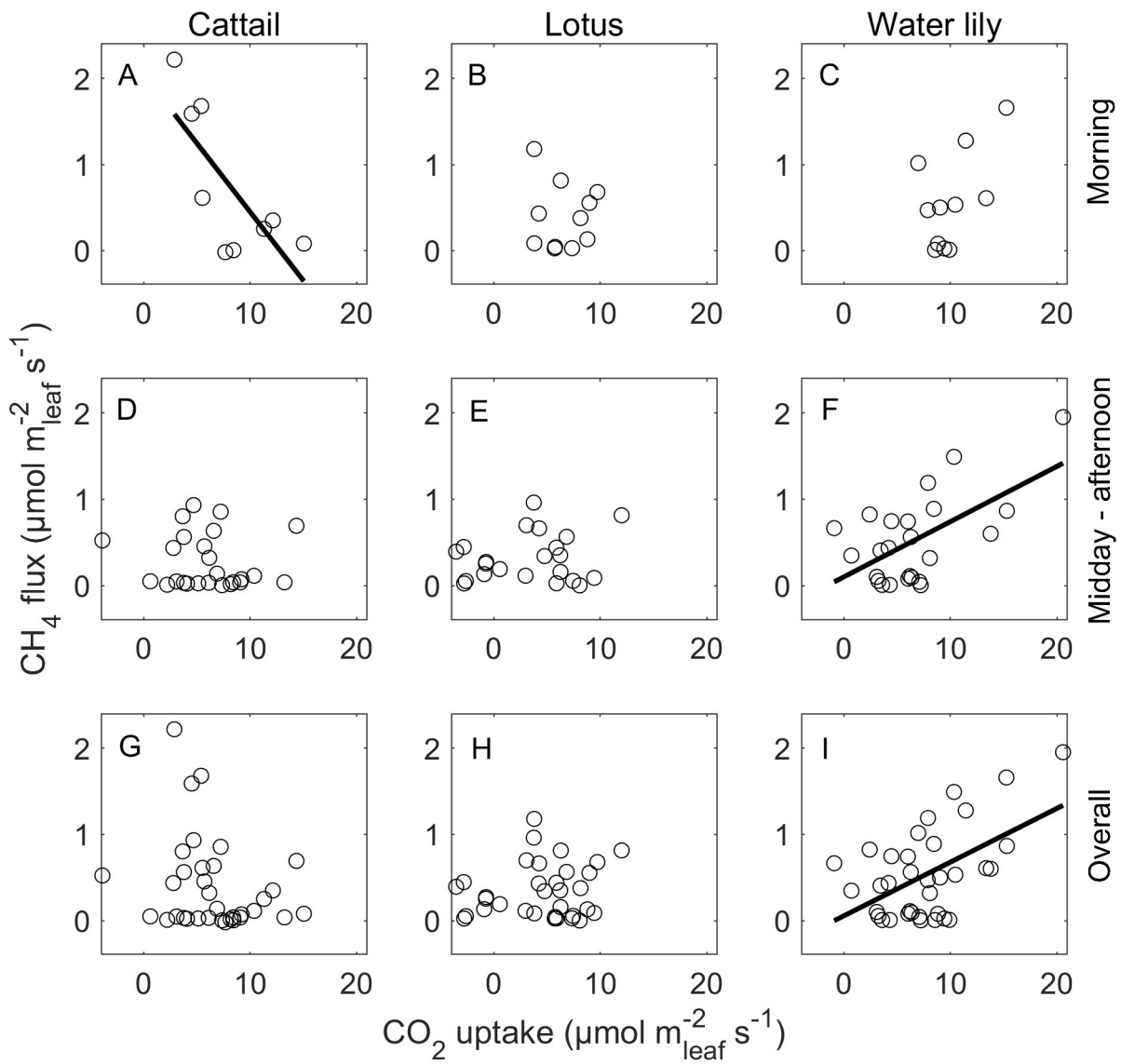lno_11467_figure 1.eps
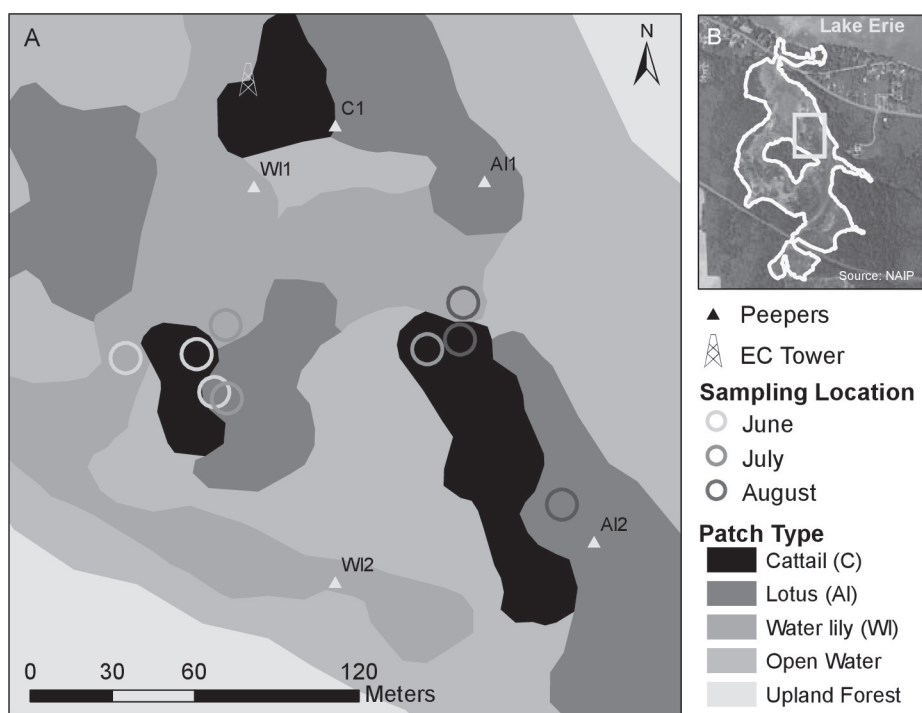
lno_11467_figure 1_bw.eps

LNO_11467_Figure 2.tif

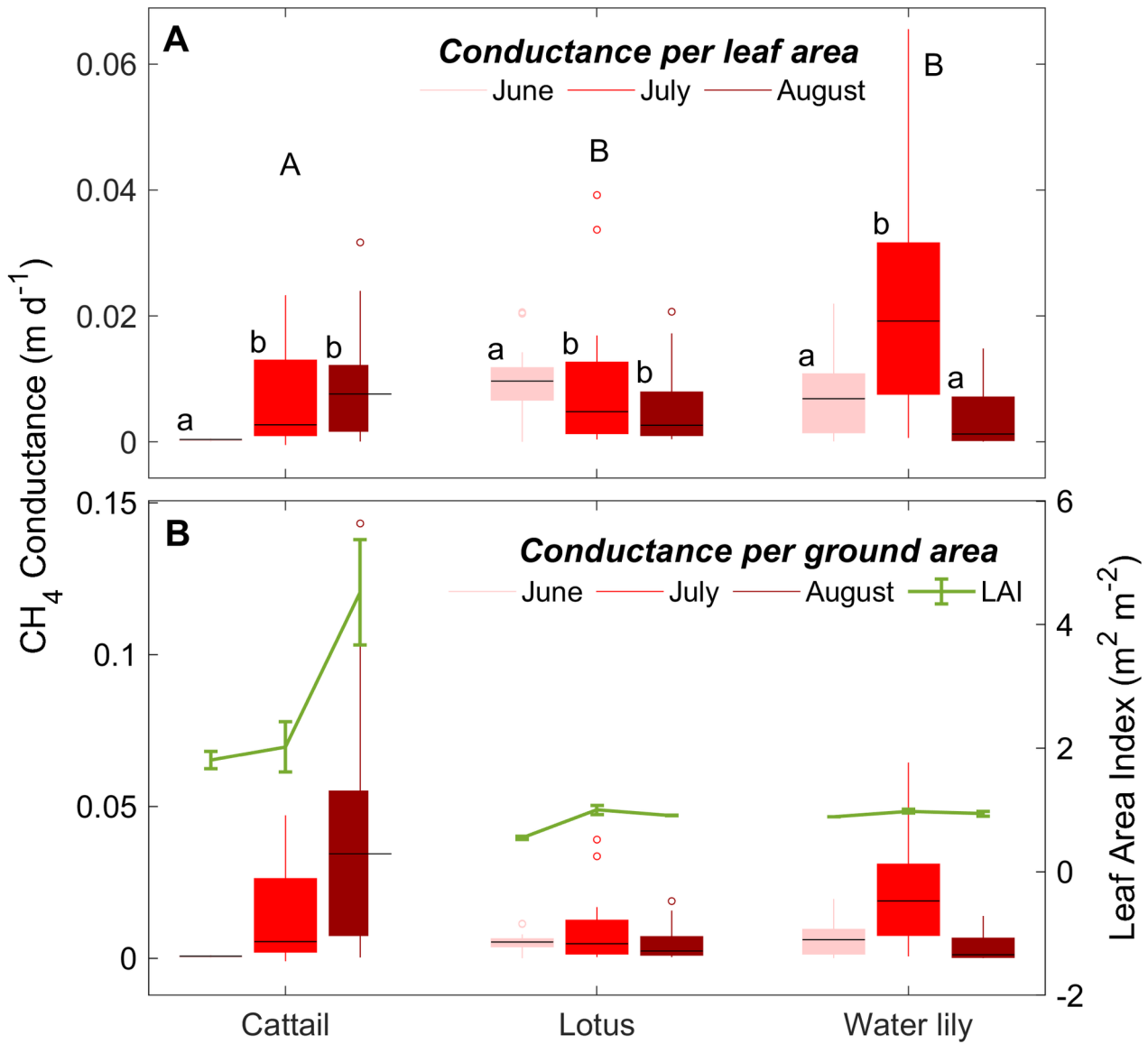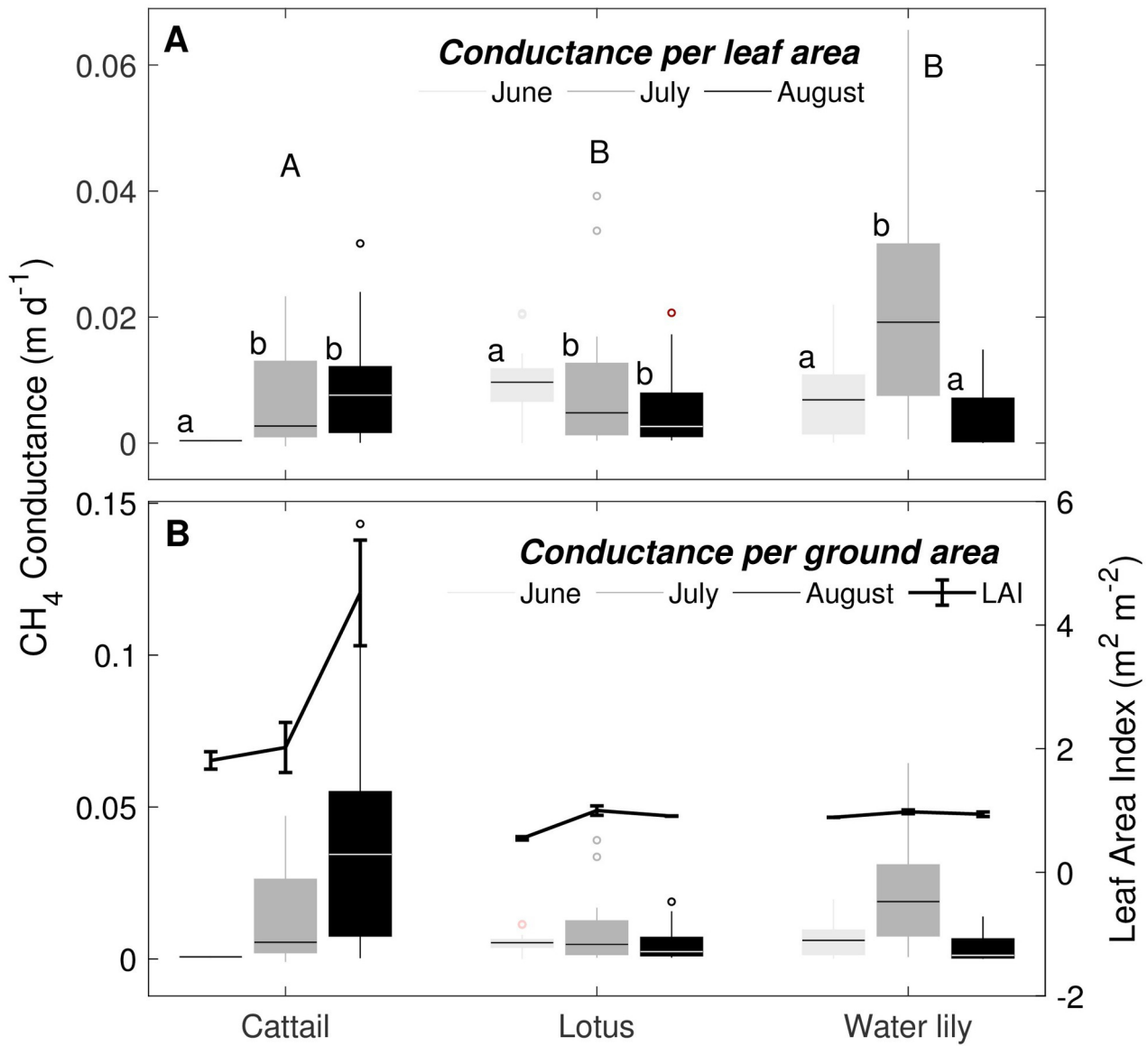lno_11467_figure 2_bw.eps

Cattail   Lotus   Water lily

A   B   C   Morning

D   E   F   Midday - afternoon

G   H   I   Overall

CH_4 flux (μmol m_{leaf}^{-2} s^{-1})

CO_2 uptake (μmol m_{leaf}^{-2} s^{-1})

LNO_11467_Figure 3.tif

Cattail   Lotus   Water lily

CH$_4$ flux (µmol m$_{leaf}^{-2}$ s^{-1})

CO$_2$ uptake (µmol m$_{leaf}^{-2}$ s^{-1})
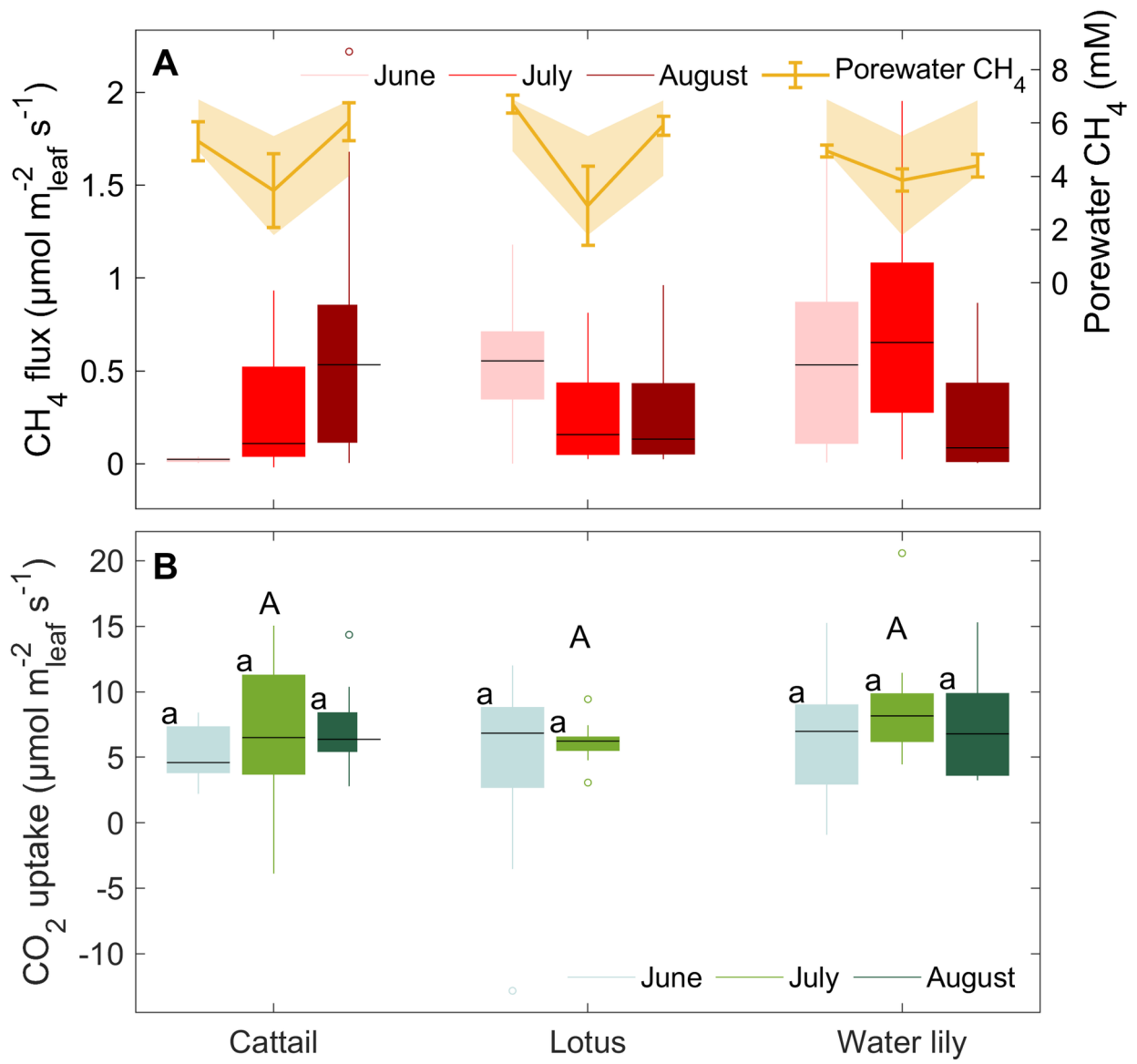
Morning

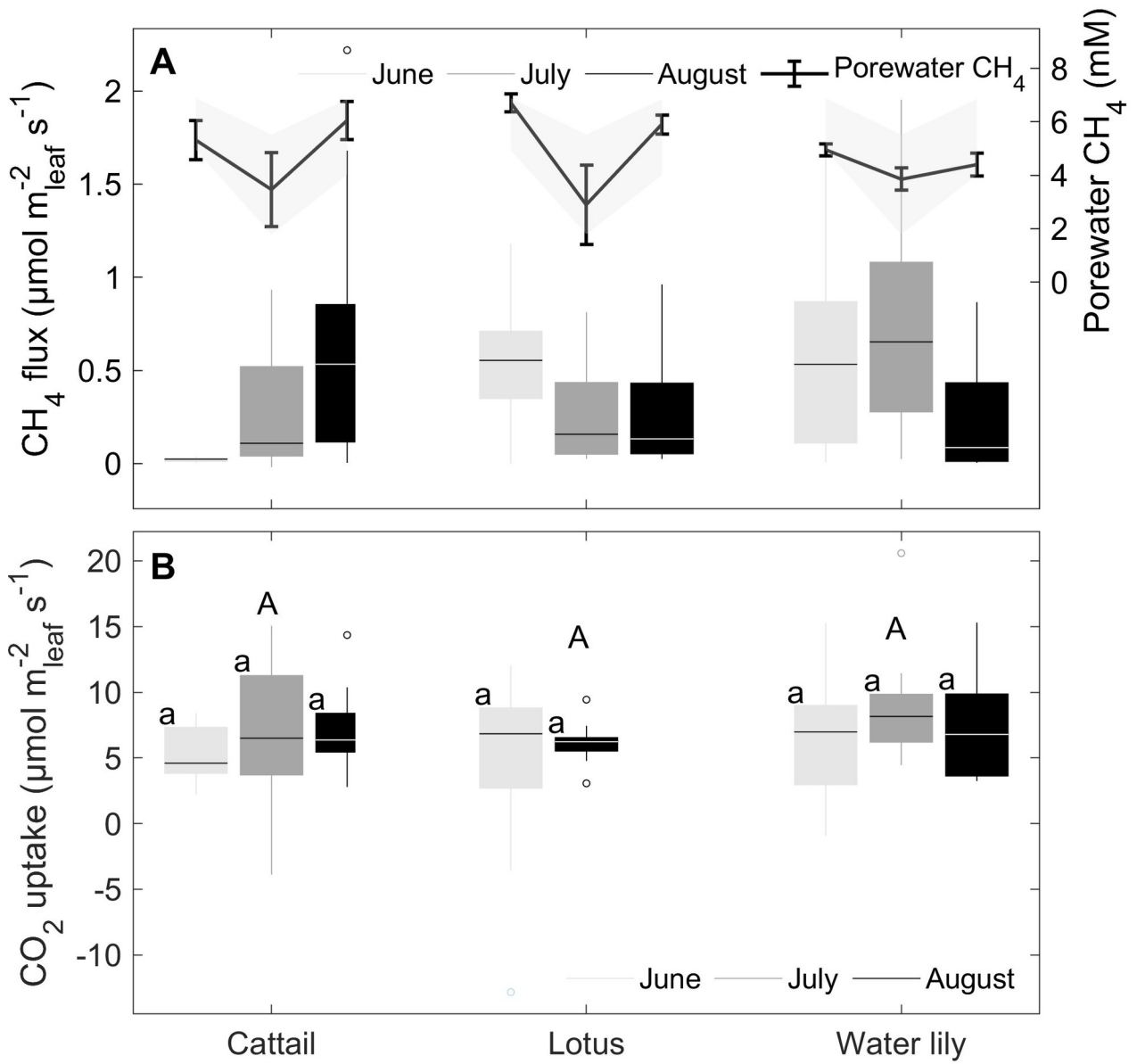Midday - afternoon

Overall

lno_11467_figure 3_bw.eps

LNO_11467_Figure 4.tif

lno_11467_figure 4_bw.eps

LNO_11467_Figure 5.tif

lno_11467_figure 5_bw.eps